Protein Tyrosine Phosphatase, Shp2, Positively Regulates Macrophage Oxidative Burst

Xing Jun Li[1,2], Charles B Goodwin[2,3], Sarah C. Nabinger[3], Briana M. Richine[2,3], Zhenyun

Yang[4], Helmut Hanenberg[1,2,3,5], Hiroshi Ohnishi[6], Takashi Matozaki[7], , Gen-Sheng Feng[8],

and Rebecca J. Chan[1,2,3]

[1]Department of Pediatrics, [2]Herman B Wells Center for Pediatric Research, [3]Department of

Medical & Molecular Genetics, Indiana University School of Medicine, Indianapolis, IN, USA

[4]West Coast University, Los Angeles, CA, USA

[5]Department of Otorhinolaryngology and Head/Neck Surgery, Heinrich Heine University,

Düsseldorf, Germany

[6]Gunma University Graduate School of Health Sciences, Maebashi, Gunma, JP

[7]Kobe University Graduate School of Medicine, Chuo-Ku, Kobe, JP

[8]Department of Pathology, UC San Diego, La Jolla, CA, USA

*Running title: *Functional and Mechanistic Contribution of Shp2 to Oxidative Burst*

To whom correspondence should be addressed: Xing Jun Li or Rebecca J. Chan, Department of Pediatrics, Indiana University School of Medicine, Indianapolis, IN, USA, Tel.: 317-274-4719; Fax: 317-278-8679; E-mail: xl9@iu.edu or rchan@iu.edu

Background: Innate immune cell oxidative burst is needed to combat pathogens.
Results: Loss of Shp2 phosphatase reduces, while increased Shp2 phosphatase function enhances ROS production.
Conclusion: The Shp2 phosphatase domain is specifically required for optimal oxidative burst in macrophages.

Significance: Humans bearing aberrancies of Shp2 phosphatase or of Shp2-containing signaling pathways may be prone to impaired or excessive ROS production.

ABSTRACT
Macrophages are vital to innate immunity, and express pattern recognition receptors and

integrins for the rapid detection of invading pathogens. Stimulation of Dectin-1 and complement receptor 3 (CR3) activates Erk- and Akt-dependent production of reactive oxygen species (ROS). Shp2, a protein tyrosine phosphatase encoded by *Ptpn11*, promotes activation of Ras-Erk and PI3K-Akt and is crucial for hematopoietic cell function; however, no studies have examined Shp2 function in particulate-stimulated ROS production. Maximal Dectin-1-stimulated ROS production corresponded kinetically to maximal Shp2 and Erk phosphorylation. Bone marrow derived macrophages (BMMs) from mice with a conditionally deleted allele of *Ptpn11* (Shp2$^{flox/flox}$;Mx1Cre+) produced significantly lower ROS levels compared to control BMMs. Although yellow fluorescent protein (YFP)-tagged phosphatase dead Shp2-C463A was strongly recruited to the early phagosome, its expression inhibited Dectin-1- and CR3-stimulated phospho-Erk and ROS levels, placing Shp2 phosphatase function and Erk activation upstream of ROS production. Further, BMMs expressing gain-of-function (GOF) Shp2-D61Y or Shp2-E76K and peritoneal exudate macrophages (PEMs) from Shp2D61Y/+;Mx1Cre+ mice produced significantly elevated levels of Dectin-1- and CR3-stimulated ROS which was reduced by pharmacologic inhibition of Erk. Signal regulatory protein α (SIRPα) is a myeloid inhibitory immunoreceptor that requires tyrosine phosphorylation to exert its inhibitory effect. YFP-Shp2C463A-expressing cells have elevated phospho-SIRPα levels and an increased Shp2- SIRPα interaction compared to YFP-WT Shp2-expressing cells. Collectively, these findings indicate that Shp2 phosphatase function positively regulates Dectin-1- and CR3-stimulated ROS production in macrophages by de-phosphorylating and thus mitigating the inhibitory function of SIRPα and by promoting Erk activation.

INRODUCTION

Macrophages are phagocytic cells that function as the body's global first-line defense against invading pathogens. Upon interaction with pathogen-producing stimuli, macrophages internalize large particulate microorganisms and generate microbicidal reactive oxygen species (ROS) produced by activated nicotinamide adenine dinucleotide phosphate (NADPH) oxidase (1). NADPH oxidase is composed of membrane-integrated gp91^{phox} and p22^{phox} as well as the four cytosolic components p47^{phox}, p67^{phox}, p40^{phox}, and Rac2 (2,3). Individuals with chronic granulomatous disease (CGD) have inherited germline mutations within variable components of the NADPH oxidase complex, and suffer from recurrent, life-threatening bacterial and fungal infections, highlighting the imperative nature of competent ROS production by the innate immunity (4,5).

Shp2, a protein tyrosine phosphatase encoded by the *PTPN11* gene, promotes activation of Ras-Erk signaling and plays an essential role in hematopoietic cell development (6,7). Genetic disruption of murine *Ptpn11* within hematopoietic lineages leads to rapid loss of blood cell production of all lineages (8,9). In humans, gain-of-function *PTPN11* mutations are commonly found in children with Noonan syndrome and juvenile myelomonocytic leukemia (JMML) (10,11). Although no *PTPN11* mutations have been found to be associated with clinical immune deficiency, Shp2 is a critical signaling component of Leptin Receptor-dependent protection against the parasitic pathogen, *Entamoeba histolytica* (12), and children bearing germline loss-of-function *LEPR* mutations are susceptible to respiratory infections (13). Further, previous studies found that Shp2 regulates the phosphorylation of transcription factors HoxA10 and ICSBP, leading to transcriptional repression of the NADPH oxidase components gp91^{phox} and p67^{phox} and preventing myeloid terminal differentiation (14,15); however, no studies have examined the function of Shp2 phosphatase in ROS production in terminally differentiated macrophages or neutrophils, which may reveal a novel role for Shp2 in innate immunity and ROS production.

Macrophages are capable of detecting and responding to pathogen-derived molecules such as fungal glucans and lipopolysaccharides, as they express cell surface pattern recognition receptors (PRRs) such as C-type lectins. Dectin-1 is a C-type lectin expressed on macrophages that responds to

β-glucan-containing particles derived from fungal cell walls and stimulates Src- and Syk-dependent signaling (16). Dectin-1 stimulation results in activation of the Ras-Erk pathway, production of microbicidal ROS, and induction of expression of the inflammatory cytokines, TNFα and IL6. In humans, loss-of-function mutations in *DECTIN-1* confer a state of increased susceptibility to mucocutaneous *C. albican*s and invasive aspergillosis (17,18).

Based on the known high expression of Shp2 in macrophages and its well-defined role as a positive regulator of the Ras-Erk pathway, we hypothesized that Shp2 promotes normal innate immunity by positively upregulating particulate-stimulated NADPH oxidase activation and abrupt production of ROS, known as oxidative burst. To address this hypothesis, we examined the correlation of Shp2 activation to peak ROS production in zymosan-stimulated peritoneal exudate macrophages (PEMs) and examined the putative placement of Shp2 in the Dectin-1-stimulated pathway employing genetic studies and pharmacologic studies using the Syk inhibitor, R406, and the Erk inhibitor, SCH772984. Genetic disruption of *Ptpn11* resulted in reduced macrophage ROS production in response to both zymosan (Dectin-1 stimulation) and serum opsonized zymosan (SOZ, complement receptor 3 stimulation), indicating a positive function of Shp2 in oxidative burst. Structure-function studies using various Shp2 loss-of-function and gain-of-function constructs indicated that the phosphatase function of Shp2 is specifically required for positive regulation of particulate-stimulated oxidative burst. Mechanistic studies demonstrated that Shp2 exerts its positive effect on ROS generation by de-phosphorylating the myeloid inhibitory immunoreceptor, SIRPα (signal regulatory protein α), and by promoting Erk activation.

EXPERIMENTAL PROCEDURES
Reagents. Chemicals were purchased from Sigma-Aldrich (St. Louis, MO) unless otherwise stated. Phosphate-buffered saline (PBS) pH 7.2, penicillin/streptomycin, neomycin, IMDM and DMEM were from Invitrogen Life Technologies (Carlsbad, CA); fetal calf serum (FCS) was from HyClone Laboratory (Logan, UT). The ECL detection kit came from Pierce (Rockford, IL).

Rabbit polyclonal antibody against p40^{phox} and mouse monoclonal antibody T-Syk were from Upstate Biotechnology (Lake Placid, NY), rabbit polyclonal antibody against p47^{phox} was from Santa Cruz Biotechnology (Santa Cruz, CA), and monoclonal antibody against p67phox was from BD Biosciences (Franklin Lakes, NJ). Rabbit polyclonal and mouse monoclonal antibodies against Shp2 was from Santa Cruz Biotechnology (SC-280) and BD Bioscience (#610621), respectively. Anti-SIRPα polyclonal antibody was from Abcam (#53721) and mouse dectin-1/CLEC7A antibody (Clone 218838) was from R&D Systems, Inc. (Minneapolis, MN). Anti-phospho-SIRPα was generated as previously described (19). Anti-gp91^{phox} mAb 54.1 and anti-p22^{phox} mAb NS2 were kindly provided by A. J. Jesaitis (Montana State University) (20). All the other antibodies, including anti-phospho-antibodies, were obtained from Cell Signaling Technology (Beverly, MA) unless otherwise stated. Zymosan A from *Saccharomyces cerevisiae* was from Sigma (Z-4250). The fluorescein isothiocyanate (FITC)–labeled zymosan particles were from Life Technologies. Phycoerythrin (PE)-Mac-1 and allophycocyanin (APC)-F4/80 were from BD Pharmingen.

Animal Husbandry. Mice bearing a conditional gain-of-function (GOF) *Ptpn11* allele (*LSL-Shp2$^{D61Y/+}$*) or a conditional floxed *Ptpn11* allele (*Shp2$^{flox/flox}$*) have been described (9,21,22) and were crossed with mice bearing the Mx1Cre transgene to generate experimental (Shp2D61Y;Mx1Cre+ or Shp2$^{f/f}$;MxCre+) and negative control (Shp2D61Y;Mx1Cre- or Shp2$^{f/f}$;MxCre-) animals. All animals received three intraperitoneal injections with 300 µg polyI:polyC (GE Healthcare) to induce *Ptpn11* recombination. All mice were maintained under specific pathogen-free conditions at the Indiana University Laboratory Animal Research Center (Indianapolis, IN) and this study was approved by the Institutional Animal Care and Use Committee of the Indiana University School of Medicine.

Plasmid construction. The cDNAs encoding wildtype (WT) Shp2 or Shp2-R32K and Shp2-C463A mutants were cloned into EcoRI and KpnI sites of pEYFP-N1 (Clontech; San Diego, CA) to generate yellow fluorescent protein (YFP)-tagged

3

Shp2 constructs, and the constructs were confirmed by sequencing. The YFP-tagged Shp2 cDNAs were then ligated into pMSCV (Clontech) for use in generation of retroviral supernatants. Preparation and characterization of the pMIEG3-WT Shp2, Shp2-D61Y, and Shp2-E76K was described previously (23).

Retroviral transduction of bone marrow (BM) and macrophage differentiation. Retroviral transduction of murine bone marrow low density mononuclear cells (LDMNCs, C57Bl/6 background) with MSCV-WT Shp2-YFP, Shp2-R32K-YFP, or Shp2-C463A-YFP or with MIEG3-WT Shp2, Shp2-D61Y, or Shp2-E76K was performed as described (23,24). Transduced cells were sorted by fluorescence activated cell sorting (FACSCalibur, BD; Franklin Lakes, NJ) prior to macrophage differentiation, as described (23). Activity, immunostaining, and live images were analyzed 6-7 days after macrophage differentiation.

Peritoneal exudate macrophage (PEM) preparation. Eight weeks after polyI:polyC treatment, Shp2D61Y;Mx1Cre+ and negative control Shp2D61Y;Mx1Cre- animals were injected with 1 mL of 3% thioglycollate to induce peritoneal inflammation. 72 hours later, peritoneal cells were harvested by lavage with PBS, and macrophages were isolated by culturing cells at 1×10^6 cells/mL in IMDM with 20% heat-inactivated (HIA)-serum and 2% Penicillin-Streptomycin (P/S) in a tissue culture dish for 2 hours, and then removing non-adherent cells (25). After overnight incubation in IMDM with 20% HIA-serum and 2% P/S, PEMs were used to perform functional and biochemical analyses.

Preparation of particulate stimuli. Zymosan and serum opsonized-zymosan A particles (SOZ, Sigma Z-4250) were prepared as previously described (26-28). A synchronized phagocytosis assay was used for zymosan- or SOZ-induced NADPH oxidase activity assays (29,30). Briefly, macrophages in 200 µL PBSG were incubated on ice for 5 minutes in 50 µM luminol and 20 U/mL HRP, then 25 µL cold zymosan or SOZ (final concentration: 400 µg/mL) were added. Cells and particles were spun at 1200rpm for 5 minutes at 4°C, then immediately placed at 37°C in the luminometer.

Reactive oxygen species (ROS) detected by chemiluminescence in intact cells. ROS production during synchronized phagocytosis of SOZ or zymosan stimulation was measured in the presence of 20 µM luminol with 20 U/mL horseradish peroxidase (HRP) (24,30,31). An Lmax microplate luminometer (Molecular Devices, Sunnyvale, CA) was used to record luminescence as previously described (24,26). For some experiments, macrophages were pre-incubated at 37° C with Syk inhibitor, R406, NADPH oxidase inhibitor, diphenyleneiodonium chloride (DPI), or Erk inhibitor for 30 minutes.

Phagocytosis assays. Synchronized phagocytosis was performed as previously described (24). Briefly, 2×10^6 macrophages were washed with PBS and resuspended in 3 mL PBSG, added to 6-well plate, and kept on ice for 5minutes, followed by adding 300 µL cold SOZ or zymosan (4.4 µg/µL in PBSG) for a final concentration of 400 µg/mL. Plates were immediately centrifuged at 1200 rpm for 5 min at 4°C, and then transferred to 37°C for indicated time. For biochemical studies, cells were washed in PBS X 3, and 60 µL lysis buffer was added to each well. For the phagocytic assays, the macrophages were plated at 0.5×10^6 cells/well in 12-well plates in macrophage differentiation medium incubated at 37°C for 24 hours. After washing, fluorescein isothiocyanate (FITC)–labeled zymosan particles (100 µg/mL) (Molecular Probes, Life Technologies) were added to the cells, and cells were incubated at 37°C for indicated time. The cells were then put on ice and washed thoroughly to remove unbound particles with PBS. The macrophages were detached and analyzed by flow cytometry immediately.

Western blots. Macrophages were lysed in lysis buffer containing 50 mM Hepes (pH 7.4), 150 mM NaCl, 10% glycerol, 1% Triton X-100, 1.5 mM $MgCl_2$, 1 mM EGTA,100 mM NaF, 10 mM sodium pryophosphate, 1 mM phenylmethylsulfonyl fluoride (PMSF), 1X protease inhibitor cocktail set I (Calbiochem), 1 mM Na_3VO_4, and 0.1 mM $ZnCl_2$ (32,33). 10 µg protein lysate was subjected to SDS-PAGE and immunoblotting using ECL detection (24,26). YFP expression was also analyzed by flow cytometry (FACSCalibur, BD) (24,26).

4

Immunoprecipitation (IP). 100 μg cell lysates were adjusted to a total volume of 1 mL in IP incubation buffer (50 mM Hepes, pH 7.4, 1% Triton X-100, 150 mM NaCl, 5 mM EDTA, 0.1% bovine serum albumin (BSA), 50 mM NaF, 1mM PMSF, 1X protease inhibitor cocktail set I (Calbiochem), 1 mM Na_3VO_4, and 0.1 mM $ZnCl_2$). 2 μg anti-Shp2 polyclonal antibody (SC-280, Santa Cruz Biotechnology) was added to the cell lysates and incubated at 4ºC for 1 hour, followed by addition of 25 μL Protein A/G PLUS-Agarose (Santa Cruz Biotechnology) and incubated for 2 – 3 h at 4ºC. The beads was washed three times in buffer (50 mM Hepes, pH 7.4, 1% Triton X-100, 120 mM NaCl, 5 mM EDTA, 50 mM NaF, 1 mM PMSF, 1X protease inhibitor cocktail set I (Calbiochem), 1 mM Na_3VO_4, and 0.1 mM $ZnCl_2$), resuspended in 25μL 2X SDS-PAGE loading buffer, boiled for 5 min, and supernatant was subjected to SDS-PAGE and immunoblotting with anti-phospho-SIRPα or anti-Shp2.

Immunofluorescence microscopy. Immunostaining for Shp2 was performed after synchronized phagocytosis. Briefly, 1×10^6 PEMs or BMMs in 2 mL PBSG were added to coverslip-bottomed dishes (MatTek Cultureware, Ashland, MA), and incubated for 5 min on ice prior to adding 300 μL zymosan or SOZ (final concentration 400 μg/mL). The cells and particles were spun down at 1200 rpm for 5 min at 4°C, then incubated at 37°C for 10 min for PEMs or 30min for BMMs. Phagocytosis was terminated by placing the cells on ice, which were then washed with cold PBS, fixed with 4% paraformaldehyde for 10 min at room temperature, permeabilized with 0.1% TritonX-100 in PBS, blocked with 10% goat serum plus 2% BSA in PBS, and immunostained with anti-Shp2 followed by Alexa-568 goat anti-rabbit IgG. For co-staining, cells were immunostained with anti-SIRPα polyclonal Ab (#53721, Abcam) and anti-Shp2 mAb (#610621, BD Bioscience) followed by Alexa-568 goat anti-rabbit IgG and Alexa-488 goat anti-mouse IgG1. Cells were imaged on a spinning-disk (CSU10) confocal system mounted on a Nikon TE-2000U inverted microscope with an Ixon air-cooled EMCCD camera (Andor Technology, South Windsor, CT) and a Nikon Plan Apo 100X 1.4 N.A. objective. Images shown are representative of at least 3 independent experiments.

Live cell imaging by confocal videomicroscopy. SOZ-induced phagocytosis in WT mouse BMMs expressing YFP-tagged WT Shp2, Shp2-C463A, or Shp2-R32K was filmed using a spinning-disk (CSU10) confocal system mounted on a Nikon TE-2000U inverted microscope with an Ixon air-cooled EMCCD camera (Andor Technology, South Windsor, CT) and a Nikon Plan Apo 100X 1.4 N.A. objective as described previously. All images were analyzed with Metamorph software (Universal Imaging; Downington, PA). Each type of experiment was performed on at least 3 independent occasions. Live images were collected in a single confocal plane (1 μM) with 514 nm excitation and 0.3 sec exposure with a time lapse of 10 sec.

Statistical Analysis. Groups were compared using unpaired, two-tailed, Student's *t* test.

RESULTS

Shp2 functions downstream of Syk in Dectin-1 signaling. Previous work has demonstrated that Dectin-1 stimulation with β-glucan-containing particles leads to Ras-Erk pathway activation and ROS production in a Syk-dependent manner (16). Given that the protein tyrosine phosphatase, Shp2, positively regulates Ras-Erk pathway signaling and is known to be crucial for normal hematopoietic cell development and function (6,7), we hypothesized that Shp2 functions in the Dectin-1 signaling pathway to promote particulate-stimulated ROS production in macrophages. To address this hypothesis, we used peritoneal exudate macrophages (PEMs) to examine the kinetics of Shp2 phosphorylation at tyrosine 580 (Y580, indicating that Shp2 is in its open, active conformation) (34) in response to zymosan, and correlated Shp2 phosphorylation with peak ROS production and activation of the known Dectin-1-responsive signaling molecules, Syk, Erk, and Akt. Zymosan exposure induced maximal ROS production at 10 minutes post-stimulation, and this time point corresponded to maximal activation of Syk, Shp2, and Erk (Figs. 1A and 1B). As expected, Akt was also activated by zymosan stimulation; however, peak Akt activation was at one hour post-stimulation, and after the peak ROS production, suggesting that Akt serves to support sustained ROS production rather than promoting

5

immediate and maximal ROS production. Upon treatment with the Syk inhibitor, R406, ROS production was strongly suppressed, which correlated kinetically with reduced Syk, Shp2, Erk, and Akt activation (Figs. 1C and 1D). Importantly, R406 treatment did not suppress expression of p22^{phox} and gp91^{phox}, (Figs. 1D), suggesting that reduced ROS is not due to altered expression of NADPH oxidase components, but is instead due to reduced NADPH oxidase function.

Genetic disruption of Shp2 results in reduced zymosan- and serum opsonized zymosan (SOZ)-stimulated ROS production. We next used a mouse model bearing a conditionally floxed allele of *Ptpn11* (Shp2$^{f/f}$;Mx1Cre+) (9). Shp2$^{f/f}$;Mx1Cre+ and negative control Shp2$^{f/f}$;Mx1Cre- mice were treated with 300 µg polyI:polyC every other day for 3 doses. Four – six weeks following polyI:polyC treatment, animals were euthanized followed by isolation of bone marrow low density mononuclear cells (LDMNCs) which were cultured in M-CSF to generate bone marrow-derived macrophages (BMMs). Based on Mac1 and F4/80 staining, cultured BMMs from the Shp2$^{f/f}$;Mx1Cre+ and Shp2$^{f/f}$;Mx1Cre- mice demonstrated a similar level of terminal differentiation (Fig. 2A). However, following stimulation with zymosan (Dectin-1 stimulation) or with SOZ (CR3 stimulation), the Shp2$^{f/f}$;Mx1Cre+ BMMs demonstrated a reduced oxidative burst compared to the Shp2$^{f/f}$;Mx1Cre- BMMs (Figs. 2B, 2C, and 2D). As Shp2 had previously been found to regulate FcγR-induced phagocytosis in macrophages (35), we next examined if the reduced ROS production was due to a global reduction in phagocytosis; however, the phagocytic index was similar for the Shp2$^{flox/flox}$;Mx1Cre+ and Shp2$^{flox/flox}$;Mx1Cre- BMMs (Fig. 2E). Moreover, we found that expression of various components of the NADPH oxidase complex (p22^{phox}, gp91^{phox}, p40^{phox}, p47^{phox}, p67^{phox}) were expressed at similar levels in the Shp2$^{f/f}$;Mx1Cre+ and Shp2$^{f/f}$;Mx1Cre- BMMs (Fig. 2F), indicating that the reduced ROS seen in the Shp2$^{flox/flox}$;Mx1Cre+ BMMs is not due to reduced expression of *phox* proteins.

When examining Dectin-1 signaling, both total Shp2 and phospho-Shp2 levels were reduced in the Shp2$^{f/f}$;Mx1Cre+ BMMs, and as anticipated Erk activation was reduced in a correlative fashion (Fig.

2G). Reduced Shp2 expression did not have an effect on overall phospho-Akt levels, suggesting that the Shp2-regulated Erk activation is more relevant to abrupt and maximal ROS production. Consistent with the pharmacologic data using R406, reduced Shp2 expression and activation did not cause reduced activation of Syk. Collectively, these functional and biochemical studies suggest that Shp2 functions downstream of Syk in the Dectin-1-stimulated signaling pathway, and positively upregulates Dectin-1-stimulated ROS levels.

Shp2 is recruited to the phagosome and requires tyrosine phosphatase function to promote ROS production. Given the positive role of Shp2 on zymosan- and SOZ-stimulated ROS production, we next imaged SOZ-stimulated BMMs to determine if Shp2 is recruited to the phagosome membrane, the location of the NADPH oxidase complex. Consistent with the positive functional findings, we found that Shp2 strongly co-localizes with F-actin on the phagosomal cup and early phagosomes (Fig. 3A).

To define the biochemical role of Shp2 in ROS production, we generated yellow fluorescent protein (YFP)-tagged Shp2 constructs bearing mutation of the N-SH2 (R32K) or phosphatase (C463A) domains (Fig. 3B). These constructs were retrovirally introduced into murine bone marrow LDMNCs followed by sorting to enrich for YFP+ cells and generation of bone marrow-derived macrophages (BMMs). Sorted, differentiated macrophages expressed similar levels of each of the Shp2 constructs based on YFP expression (Fig. 3C) and immunoblot analysis (Fig. 3D), expressed similar levels of the NADPH oxidase components, p67^{phox}, p22^{phox}, and gp91^{phox} (Fig. 3D), and differentiated similarly based on Mac1 and F4/80 expression (Fig. 3E). When subjected to zymosan or SOZ stimulation, mutation of either the N-SH2 domain or the phosphatase domain resulted in reduced ROS production (Fig. 3F). Given the functional effect of the N-SH2 domain and phosphatase dead mutants, we next compared the subcellular phagosomal membrane localization of WT Shp2 to the point mutants using time-lapse confocal videomicroscopy. The N-SH2 domain mutant was not recruited to the phagosome; however, the phosphatase dead mutant was strongly

recruited to the phagosome, even more intensely than WT Shp2 (Fig. 3G). These findings suggest that the phosphatase function of Shp2 specifically is needed for the positive regulation of NADPH oxidase.

Gain-of-function (GOF) Shp2 mutants enhance zymosan- and SOZ-stimulated ROS production. Based on the finding that expression of phosphatase dead Shp2-C463A resulted in reduced ROS production, we reasoned that macrophages expressing JMML-associated GOF Shp2 mutants (10,23), characterized to have increased phosphatase activity (10,36), would produce elevated zymosan- and SOZ-stimulated ROS levels. To examine this hypothesis, we retrovirally introduced WT Shp2, Shp2-D61Y, or Shp2-E76K into murine bone marrow LDMNCs followed by in vitro differentiation to BMMs. We demonstrated increased total Shp2 expression (compared to vector-transduced cells, Fig. 4A); however, the NADPH oxidase protein components were similar in all cells (Fig. 4A). As anticipated, BMMs retrovirally expressing GOF Shp2-D61Y or GOF Shp2-E76K produced significantly elevated levels of ROS in response to zymosan and SOZ compared to BMMs retrovirally expressing WT Shp2 (Fig. 4B and 4C). Additionally, Shp2-D61Y was strongly recruited to the SOZ-stimulated phagosomal cup and early phagosome, similar to that seen with WT Shp2 (Fig. 4D).

To utilize a more physiologic model, we examined ROS production using PEMs from Shp2D61Y;Mx1Cre+ mice, in which Shp2D61Y is under the endogenous control of the *Ptpn11* promoter (21). PEMs collected from the Shp2D61Y;Mx1Cre- and Shp2D61Y;Mx1Cre+ mice demonstrated a similar level of terminal differentiation based on F4/80 and Mac1 staining (Fig. 5A) and expressed similar levels of the NADPH oxidase components, p40^{phox}, p22^{phox}, and gp91^{phox} (Fig. 5E). Consistent with the retrovirally transduced cells, PEMs from Shp2D61Y;Mx1Cre+ mice produced substantially higher levels of zymosan- and SOZ-stimulated ROS compared to PEMs from Shp2D61Y;Mx1Cre- mice (Fig. 5B, 5C, and 5D). Using Shp2D61Y;Mx1Cre+ PEMs, we interrogated the Dectin-1-stimulated signaling pathway to further clarify the contribution of Syk, Shp2, Erk, and Akt activation to the elevated ROS

production in response to zymosan. As predicted, we found increased phospho-Shp2 and enhanced Erk activation in the GOF Shp2-expressing cells compared to control cells (Fig. 5E). Akt activation was not substantially elevated in the Shp2D61Y-expressing cells, suggesting Shp2 regulation of Erk activation is more relevant for zymosan-induced maximal ROS production. Interestingly, Erk activation was sustained longer in these cells compared to that observed using WT PEMs (Fig. 1) or the bone marrow-derived macrophages from Shp2$^{f/f}$;MxCre- mice (Fig. 2). This difference in Erk inactivation kinetics might be due to a strain difference of the Shp2D61Y;Mx1Cre animals, which are on a mixed C57Bl/6-Sv129 background rather than a pure C57Bl/6 background. Notwithstanding, these findings are consistent with the need for Erk to be activated for maximal ROS production, however, suggest that Erk inactivation is not imperative for the return of ROS to baseline levels. Consistent with previous results using R406 (Fig. 1) and Shp2$^{f/f}$;Mx1Cre+ BMMs (Fig. 2), Syk activation was not altered in the presence of GOF Shp2D61Y (Fig. 5E), again suggesting that Shp2 functions downstream of Syk in the Dectin-1 signaling pathway. Together, these findings support a model placing Shp2 downstream of Syk in Dectin-1 signaling and indicate that Shp2 phosphatase function positively regulates NADPH oxidase activity via promoting Erk activation.

Erk activation promotes ROS production in response to zymosan stimulation. Several previous studies have found that ROS *per se* functions as a signaling molecule to promote Erk activation (37). These studies were performed in non-phagocytic cells, and typically the cells were cultured in supra-physiologic concentrations of H$_2$O$_2$. On the other hand, other studies demonstrate that Erk promotes NADPH oxidase activation and ROS production (38-40). To determine if Erk activation is upstream or downstream of ROS in zymosan-stimulated macrophages, we first examined zymosan-stimulated Erk activation in the presence of the conventional NADPH oxidase inhibitor, DPI. Although incubation with DPI essentially obliterated zymosan-stimulated ROS, Erk activation was unchanged (Figs. 6A – 6C). In concordance with these findings, bone marrow derived macrophages from X-CGD mice (gp91phox-/-) (41), which are devoid of ROS

7

production, also demonstrated no change in zymosan-stimulated phospho-Erk levels (data not shown). We next treated cells with the Erk inhibitor, SCH772984, and found a significant reduction of ROS which correlated with reduced Erk activation (Figs. 6A, 6B, and 6C), suggesting that Erk functions upstream of zymosan-stimulated oxidative burst. To further define the linear arrangement of Shp2, Erk, and ROS production, we examined the effect of Erk inhibition on ROS production in Shp2D61Y-expressing macrophages. Hyperactivated Erk in Shp2D61Y-expressing macrophages was reduced by treatment with SCH772984, similar to that observed with WT Shp2-expressing macrophages (Fig. 6D). In a corresponding manner, inhibition with SCH772984 reduced the enhanced ROS levels in the zymosan-stimulated Shp2D61Y-expressing macrophages to near WT levels (Fig. 6E and 6F). These findings support the hypothesis that Erk is downstream of Shp2 and upstream of NADPH oxidase and ROS production in zymosan-stimulated macrophages.

Shp2 and phospho-SIRPα co-localize on phagosomes and interact biochemically in Dectin-1-stimulated cells. Given the positive role of Shp2 phosphatase function in promoting zymosan- and SOZ-stimulated ROS, we investigated putative Shp2 phosphatase substrates that might regulate Erk and NADPH oxidase activation. SIRPα (signal regulatory protein α) is a myeloid inhibitory immunoreceptor highly expressed on macrophages, requires tyrosine phosphorylation to exert its inhibitory effect, and has been shown to be a physiological substrate of Shp2 phosphatase (42,43). Previous studies indicate that dephosphorylation of SIRPα leads to increased NFκB-stimulated expression of inflammatory cytokines and NADPH oxidase protein components such as gp91^{phox} (19,44). However, as we see a rapid effect of the various Shp2 mutants on ROS production independent of the time needed for NFκB-stimulated gene expression and protein synthesis, we anticipated that zymosan- or SOZ-stimulated SIRPα dephosphorylation would be correlated with NADPH oxidase activation and ROS production.

To address this hypothesis, we first examined the subcellular localization of SIRPα in zymosan-

stimulated PEMs, and found that SIRPα is strongly associated with the phagosome membrane at 10 minutes post stimulation, which correlates kinetically with zymosan-stimulated Shp2 activation and ROS production (data not shown). We next conducted co-localization studies between Shp2 and SIRPα on the phagosome membrane at peak ROS production, and found that indeed Shp2 and SIRPα co-localize on phagosome membranes (Fig. 7A). However, the actual percentage of phagosomes showing co-localization of Shp2 and SIRPα at peak ROS production was only approximately 10 – 15% of phagosomes. Given the relatively low prevalence of Shp2-SIRPα co-localization at the time of peak ROS production, as well as the previous observation that phosphatase dead Shp2-C463A remained more strongly associated with the phagosome membrane compared to WT Shp2 (Fig. 3G), we hypothesized dephosphorylation of SIRPα and disruption, rather than maintenance, of the Shp2-SIRPα interaction is needed for maximal activation of NADPH oxidase.

To examine this idea further, we examined zymosan-stimulated phospho-SIRPα levels, and correlated phospho-SIRPα with ROS production. As predicted, the phospho-SIRPα level was lowest at the time of maximal ROS production (10' post zymosan stimulation, Fig. 7B) and at the time of maximal Shp2 phosphorylation (Fig. 1B). If SIRPα is a substrate of Shp2 in response to phagocytic stimuli, we predicted that cells expressing phosphatase dead Shp2-C463A would demonstrated elevated phospho-SIRPα levels in response to Dectin-1 stimulation. Accordingly, we found substantially higher levels of phospho-SIRPα at baseline and in response to zymosan stimulation in the Shp2-C462A-expressing BMMs compared to the WT Shp2-expressing cells (Fig. 7C). Importantly, the elevated levels of phospho-SIRPα correlated to reduced levels of phospho-Erk (Fig. 7C), suggesting that Shp2 dephosphorylation of SIRPα constrains the SIRPα inhibitory function to permit normal Erk activation.

These findings support a model whereby Shp2 interacts with phosphorylated SIRPα, and that upon SIRPα dephosphorylation, Shp2 is released and available to augment activation of the Ras-Erk pathway, promote association of the NADPH

oxidase protein complex, and enhance production of ROS. To address this hypothesis, we performed co-immunoprecipitation (co-IP) assays to examine the interaction between phospho-SIRPα and WT Shp2 compared to Shp2-C463A. While we did observe an interaction between WT Shp2 and phospho-SIRPα (Fig. 7D), this interaction was in fact difficult to detect and required the use of approximately 3-fold more protein lysate for the co-IP compared to the amount of lysate used to detect the very strong interaction between Shp2-C463A and phospho-SIRPα (Fig. 7D). The modest biochemical interaction observed between WT Shp2 and phospho-SIRPα is consistent with the relatively low number of phagosomes demonstrating WT Shp2 – SIRPα co-localization upon zymosan stimulation (Fig. 7A), and supports the notion that Shp2 de-phosphorylation of SIRPα and disruption of the Shp2-SIRPα interaction is needed for optimal activation of Erk and NADPH oxidase.

DISCUSSION

Innate immune cell production of microbicidal ROS in response to foreign stimuli is vital for clearance of invading pathogens and immunocompetence. However, ROS production needs to be regulated in a temporal and spatial manner to minimize non-specific damage to healthy tissues. Within this manuscript, we have demonstrated that the protein tyrosine phosphatase, Shp2, is a novel player in the Dectin-1-stimulated signaling pathway and functions downstream of Syk and upstream of Erk to promote NADPH oxidase activation and oxidative burst. Further, we found that Shp2 activation and dephosphorylation of the inhibitory immunoreceptor, SIRPα, correlates kinetically with peak ROS production in Dectin-1-stimulated macrophages.

Shp2 is highly expressed in hematopoietic cells and has previously been shown to promote IL-6 production by promoting activation of NFκB (45). Additionally, Shp2 has been shown to be an important component of the Leptin Receptor signaling pathway in protecting against the parasite *E. histolytica*, and a component of this protection is due to STAT3-regulated IL-6 production (12). However, the role of Shp2 in oxidative burst has never been described. We first found that cells bearing genetic disruption of *Ptpn11* produce lower levels of zymosan- and SOZ-stimulated ROS. Using a series of Shp2 point mutants, we found that both the N-SH2 domain and the phosphatase domain of Shp2 are needed for zymosan- and SOZ-stimulated ROS. Importantly, videomicroscopy demonstrated that Shp2-R32K (N-SH2 domain mutant) failed to be recruited to the phagosome, while phosphatase dead Shp2-C463A was strongly recruited to phagosomes and was retained more intensely than WT Shp2 (Fig. 3G). These findings indicate that the N-SH2 domain is needed for Shp2 recruitment to the phagosome, however, once recruited, the phosphatase function of Shp2 is needed to promote ROS production. Supporting this idea, GOF Shp2 mutants Shp2-D61Y and Shp2-E76K increased both zymosan- and SOZ-stimulated ROS (Figs. 4 and 5).

Given the apparent positive functional role of Shp2 phosphatase on ROS production and the kinetic correlation of Erk activation with maximal ROS production (Fig. 1A and 1B), we reasoned that Shp2 exerts its positive effect on NADPH oxidase activation via positive regulation of Erk, as Shp2 has been shown to positively upregulate Erk activation in response to multiple stimuli (34,46,47). This notion is consistent with previous studies that have demonstrated positive regulation of Erk activation on NADPH oxidase (38-40). We found that the Erk inhibitor, SCH772984, reduced ROS production in both WT cells and in cells expressing GOF Shp2D61Y (Fig. 6), placing Erk downstream of Shp2 and upstream ROS production.

We next interrogated potential Shp2 substrates that may be involved in the regulation of particulate-stimulated Erk activation and ROS production. SIRPα, also known as SHPS-1/BIT/CD172a, was first identified as a phosphorylated glycoprotein that interacted with Shp2 in response to insulin stimulation, and expression of catalytically inactive Shp2 resulted in increased tyrosine phosphorylation of SIRPα (48). SIRPα contains extracellular immunoglobulin-like domains and four intracellular tyrosine residues followed by amino acid sequence XX(L/V/I), indicating sites of tyrosine phosphorylation (43). Several studies indicate that SIRPα may be a physiological substrate for Shp2 (42,43). Early functional studies

9

in fibroblasts indicated that over-expression of SIRPα inhibited receptor tyrosine kinase- and cytokine receptor-stimulated cell proliferation, and that the intracellular tyrosine residues were vital for the SIRPα inhibitory function (42). Given the high expression level of SIRPα in macrophages, investigators found that SIRPα negatively modulates inflammatory cytokine production via downregulation of NFκB-regulated expression (19,49). Additionally, one study found that SIRPα phosphorylation functioned to inhibit soluble stimulation (PMA)-induced plasma membrane ROS by down-regulating expression of the NADPH oxidase component, gp91^{phox} (44).

To date, however, no previous studies have identified SIRPα as an important regulatory molecule in particulate-stimulated oxidative burst. We first defined that SIRPα is indeed present on early phagosomal membranes in response to zymosan stimulation with similar kinetics to Shp2 phagosomal recruitment. In fluorescent microscopy studies, however, while we found that Shp2 and SIRPα co-localize on the early phagosome (Fig. 7A), we were surprised to find that the co-localization was modest and seen in only approximately 10 – 15% of phagosomes at the time corresponding to maximal ROS production (10 minutes post-stimulation). These findings suggest that SIRPα phosphorylation recruits Shp2 to the phagosome membrane, and that the Shp2-SIRPα interaction delays the full oxidative burst by sequestering Shp2 from the Ras-Erk pathway and thus deferring maximal Erk activation and ROS production. The increased association of phosphatase-dead Shp2-C463A with the phagosome (Fig. 3G) and the increased biochemical interaction between Shp2-C463A and SIRPα (Fig. 7D) in conjunction with reduced ROS production support this model.

While our data support a positive role for Shp2 phosphatase in particulate-stimulated ROS production by dephosphorylating and thus repressing the inhibitory role of SIRPα, it is important to put these findings into context with previous studies in this signaling pathway. First, studies from the Eklund lab demonstrated that Shp2 functions to de-phosphorylate the transcription factors ICSBP and HoxA10 resulting in reduced

transcription and expression of the NADPH oxidase protein components gp91^{phox} and p67^{phox} (14,15). These studies very nicely provide a rational mechanism of how GOF Shp2 mutants may inhibit expression of genes needed for myeloid cell terminal differentiation, and thus promote leukemogenesis.

Additionally, van Beek *et al*. demonstrated that ectopic expression of SIRPα in PLB-985 cells functioned in an inhibitory manner by repressing gp91^{phox} expression during granulocytic or monocytic differentiation, leading to reduced soluble stimulation (PMA)-induced ROS (44). Notably, these previous studies were performed in undifferentiated or differentiating myeloid cells, while our studies were performed in terminally differentiated macrophages. Importantly, in terminally differentiated macrophages, we did not find a difference in expression of the various NADPH oxidase components in cells lacking Shp2 (Fig. 2), expressing loss-of-function Shp2 mutants (Fig. 3), or gain-of-function Shp2 mutants (Figs. 4 & 5). Contrasting our studies to this previous work highlights an interesting concept that in undifferentiated myeloid cells, Shp2 and SIRPα may be more important for regulating transcription factor function and myeloid cell differentiation (50,51), while in terminally differentiated cells, Shp2 and SIRPα are more important for regulating phosphorylation and subcellular localization, respectively, of cytoplasmic signaling proteins.

Further, while many studies focus on the inhibitory role of SIRPα in myeloid cell immune function, others have found that SIRPα can also play a positive role in immune cell function (52). Importantly, this positive regulatory role of SIRPα was found in the context of Shp1-expressing hematopoietic cells, while many of the original studies defining a negative regulatory role of SIRPα were performed in fibroblasts which express only Shp2 (52). As both Shp1 and Shp2 are expressed in hematopoietic cells and have both been found to interact with SIRPα, and as Shp1 is conventionally thought to play a negative regulatory role and Shp2 is thought to play a positively regulatory role in hematopoietic cell function, these considerations bring into relief the speculative idea that Shp1 may function to

dephosphorylate and inhibit the positive regulatory role of SIRPα (leading to a net negative signal), while Shp2 may function to dephosphorylate and inhibit the negative regulatory role of SIRPα (leading to a net positive signal). Although beyond the point of the current study, it may be of interest to compare the effect of phosphatase dead Shp1 to that of phosphatase dead Shp2 in particulate-stimulated ROS production in terminally differentiated macrophages or neutrophils.

Based on our findings within the current study, we have clarified a model that places Shp2 activation downstream of Dectin-1-stimulated Syk and upstream of Erk and ROS production (Fig. 8). Previous work defined that upon stimulation, Dectin-1 is phosphorylated (likely by members of the Src family of kinases) resulting in Syk recruitment, Ras-Erk pathway activation (16), and immediate production of ROS (Fig. 8A and 8B). Findings within this manuscript demonstrate that Dectin-1 stimulation leads to activation of Shp2 in a Syk-dependent manner, and that phospho-Shp2 is recruited to phosphorylated SIRPα (Fig. 8B). Once Shp2 dephosphorylates SIRPα, Shp2 is available for additional positive regulation of the Ras-Erk pathway, leading to maximal ROS production (Fig. 8C). A potential means of Erk activation of NADPH oxidase function is phosphorylation of p47^{phox}, which has been found previously in neutrophils (40,53). It is possible that the SIRPα interaction with Shp2 defers maximal ROS production for the purpose of mitigating or preventing unwarranted ROS release to normal tissues. These findings also have application for improved understanding of the childhood leukemia, JMML, as aberrantly elevated ROS production from activating *PTPN11*-expressing innate immune cells may account for the common difficulty in clinically differentiating JMML from microbial and viral infections (54-56). Collectively, our findings demonstrate that Shp2 positively regulates oxidative burst at least in part by promoting Erk activation, and that the Shp2-SIRPα interaction may fine tune the optimal timing and location for ROS production.

11

References

1. Minakami, R., and Sumimotoa, H. (2006) Phagocytosis-coupled activation of the superoxide-producing phagocyte oxidase, a member of the NADPH oxidase (nox) family. *International journal of hematology* **84**, 193-198

2. Groemping, Y., and Rittinger, K. (2005) Activation and assembly of the NADPH oxidase: a structural perspective. *Biochem J* **386**, 401-416

3. Nauseef, W. M. (2004) Assembly of the phagocyte NADPH oxidase. *Histochemistry and cell biology* **122**, 277-291

4. Dinauer, M. C. (2005) Chronic granulomatous disease and other disorders of phagocyte function. *Hematology Am Soc Hematol Educ Program*, 89-95

5. Stasia, M. J., and Li, X. J. (2008) Genetics and immunopathology of chronic granulomatous disease. *Semin Immunopathol* **30**, 209-235

6. Qu, C. K., Shi, Z. Q., Shen, R., Tsai, F. Y., Orkin, S. H., and Feng, G. S. (1997) A deletion mutation in the SH2-N domain of Shp-2 severely suppresses hematopoietic cell development. *Mol Cell Biol* **17**, 5499-5507.

7. Qu, C. K., Yu, W. M., Azzarelli, B., Cooper, S., Broxmeyer, H. E., and Feng, G. S. (1998) Biased suppression of hematopoiesis and multiple developmental defects in chimeric mice containing Shp-2 mutant cells. *Mol Cell Biol* **18**, 6075-6082.

8. Chan, G., Cheung, L. S., Yang, W., Milyavsky, M., Sanders, A. D., Gu, S., Hong, W. X., Liu, A. X., Wang, X., Barbara, M., Sharma, T., Gavin, J., Kutok, J. L., Iscove, N. N., Shannon, K. M., Dick, J. E., Neel, B. G., and Braun, B. S. Essential role for Ptpn11 in survival of hematopoietic stem and progenitor cells. *Blood* **117**, 4253-4261

9. Zhu, H. H., Ji, K., Alderson, N., He, Z., Li, S., Liu, W., Zhang, D. E., Li, L., and Feng, G. S. Kit-Shp2-Kit signaling acts to maintain a functional hematopoietic stem and progenitor cell pool. *Blood* **117**, 5350-5361

10. Tartaglia, M., Niemeyer, C. M., Fragale, A., Song, X., Buechner, J., Jung, A., Hahlen, K., Hasle, H., Licht, J. D., and Gelb, B. D. (2003) Somatic mutations in PTPN11 in juvenile myelomonocytic leukemia, myelodysplastic syndromes and acute myeloid leukemia. *Nature genetics* **34**, 148-150

11. Tartaglia, M., Mehler, E. L., Goldberg, R., Zampino, G., Brunner, H. G., Kremer, H., van der Burgt, I., Crosby, A. H., Ion, A., Jeffery, S., Kalidas, K., Patton, M. A., Kucherlapati, R. S., and Gelb, B. D. (2001) Mutations in PTPN11, encoding the protein tyrosine phosphatase SHP-2, cause Noonan syndrome. *Nature genetics* **29**, 465-468

12. Mackey-Lawrence, N. M., and Petri, W. A., Jr. (2012) Leptin and mucosal immunity. *Mucosal immunology* **5**, 472-479

13. Farooqi, I. S., Wangensteen, T., Collins, S., Kimber, W., Matarese, G., Keogh, J. M., Lank, E., Bottomley, B., Lopez-Fernandez, J., Ferraz-Amaro, I., Dattani, M. T., Ercan, O., Myhre, A. G., Retterstol, L., Stanhope, R., Edge, J. A., McKenzie, S., Lessan, N., Ghodsi, M., De Rosa, V., Perna, F., Fontana, S., Barroso, I., Undlien, D. E., and O'Rahilly, S. (2007) Clinical and molecular genetic spectrum of congenital deficiency of the leptin receptor. *N Engl J Med* **356**, 237-247

14. Lindsey, S., Huang, W., Wang, H., Horvath, E., Zhu, C., and Eklund, E. A. (2007) Activation of SHP2 protein-tyrosine phosphatase increases HoxA10-induced repression of the genes encoding gp91(PHOX) and p67(PHOX). *J Biol Chem* **282**, 2237-2249

15. Zhu, C., Lindsey, S., Konieczna, I., and Eklund, E. A. (2008) Constitutive activation of SHP2 protein tyrosine phosphatase inhibits ICSBP-induced transcription of the gene encoding gp91PHOX during myeloid differentiation. *J Leukoc Biol* **83**, 680-691

16. Goodridge, H. S., Underhill, D. M., and Touret, N. (2012) Mechanisms of Fc receptor and dectin-1 activation for phagocytosis. *Traffic* **13**, 1062-1071

17.   Cunha, C., Di Ianni, M., Bozza, S., Giovannini, G., Zagarella, S., Zelante, T., D'Angelo, C., Pierini, A., Pitzurra, L., Falzetti, F., Carotti, A., Perruccio, K., Latge, J. P., Rodrigues, F., Velardi, A., Aversa, F., Romani, L., and Carvalho, A. (2010) Dectin-1 Y238X polymorphism associates with susceptibility to invasive aspergillosis in hematopoietic transplantation through impairment of both recipient- and donor-dependent mechanisms of antifungal immunity. *Blood* **116**, 5394-5402

18.   Ferwerda, B., Ferwerda, G., Plantinga, T. S., Willment, J. A., van Spriel, A. B., Venselaar, H., Elbers, C. C., Johnson, M. D., Cambi, A., Huysamen, C., Jacobs, L., Jansen, T., Verheijen, K., Masthoff, L., Morre, S. A., Vriend, G., Williams, D. L., Perfect, J. R., Joosten, L. A., Wijmenga, C., van der Meer, J. W., Adema, G. J., Kullberg, B. J., Brown, G. D., and Netea, M. G. (2009) Human dectin-1 deficiency and mucocutaneous fungal infections. *N Engl J Med* **361**, 1760-1767

19.   Miyake, A., Murata, Y., Okazawa, H., Ikeda, H., Niwayama, Y., Ohnishi, H., Hirata, Y., and Matozaki, T. (2008) Negative regulation by SHPS-1 of Toll-like receptor-dependent proinflammatory cytokine production in macrophages. *Genes Cells* **13**, 209-219

20.   Taylor, R. M., Burritt, J. B., Baniulis, D., Foubert, T. R., Lord, C. I., Dinauer, M. C., Parkos, C. A., and Jesaitis, A. J. (2004) Site-specific inhibitors of NADPH oxidase activity and structural probes of flavocytochrome b: characterization of six monoclonal antibodies to the p22phox subunit. *Journal of immunology* **173**, 7349-7357

21.   Chan, G., Kalaitzidis, D., Usenko, T., Kutok, J. L., Yang, W., Mohi, M. G., and Neel, B. G. (2009) Leukemogenic Ptpn11 causes fatal myeloproliferative disorder via cell-autonomous effects on multiple stages of hematopoiesis. *Blood* **113**, 4414-4424

22.   Zhang, E. E., Chapeau, E., Hagihara, K., and Feng, G. S. (2004) Neuronal Shp2 tyrosine phosphatase controls energy balance and metabolism. *Proc Natl Acad Sci U S A* **101**, 16064-16069

23.   Chan, R. J., Leedy, M. B., Munugalavadla, V., Voorhorst, C. S., Li, Y., Yu, M., and Kapur, R. (2005) Human somatic PTPN11 mutations induce hematopoietic-cell hypersensitivity to granulocyte-macrophage colony-stimulating factor. *Blood* **105**, 3737-3742

24.   Li, X. J., Marchal, C. C., Stull, N. D., Stahelin, R. V., and Dinauer, M. C. (2010) p47phox Phox homology domain regulates plasma membrane but not phagosome neutrophil NADPH oxidase activation. *The Journal of biological chemistry* **285**, 35169-35179

25.   Zeng, M. Y., Pham, D., Bagaitkar, J., Liu, J., Otero, K., Shan, M., Wynn, T. A., Brombacher, F., Brutkiewicz, R. R., Kaplan, M. H., and Dinauer, M. C. (2013) An efferocytosis-induced, IL-4-dependent macrophage-iNKT cell circuit suppresses sterile inflammation and is defective in murine CGD. *Blood* **121**, 3473-3483

26.   Li, X. J., Tian, W., Stull, N. D., Grinstein, S., Atkinson, S., and Dinauer, M. C. (2009) A fluorescently tagged C-terminal fragment of p47phox detects NADPH oxidase dynamics during phagocytosis. *Mol Biol Cell* **20**, 1520-1532

27.   Matute, J. D., Arias, A. A., Wright, N. A., Wrobel, I., Waterhouse, C. C., Li, X. J., Marchal, C. C., Stull, N. D., Lewis, D. B., Steele, M., Kellner, J. D., Yu, W., Meroueh, S. O., Nauseef, W. M., and Dinauer, M. C. (2009) A new genetic subgroup of chronic granulomatous disease with autosomal recessive mutations in p40 phox and selective defects in neutrophil NADPH oxidase activity. *Blood* **114**, 3309-3315

28.   Suh, C. I., Stull, N. D., Li, X. J., Tian, W., Price, M. O., Grinstein, S., Yaffe, M. B., Atkinson, S., and Dinauer, M. C. (2006) The phosphoinositide-binding protein p40phox activates the NADPH oxidase during FcgammaIIA receptor-induced phagocytosis. *J Exp Med* **203**, 1915-1925

29.   Greenberg, S., Burridge, K., and Silverstein, S. C. (1990) Colocalization of F-actin and talin during Fc receptor-mediated phagocytosis in mouse macrophages. *J Exp Med* **172**, 1853-1856

30.   Tian, W., Li, X. J., Stull, N. D., Ming, W., Suh, C. I., Bissonnette, S. A., Yaffe, M. B., Grinstein, S., Atkinson, S. J., and Dinauer, M. C. (2008) Fc gamma R-stimulated activation of the NADPH oxidase: phosphoinositide-binding protein p40phox regulates NADPH oxidase activity after enzyme assembly on the phagosome. *Blood* **112**, 3867-3877

31.   Ellson, C. D., Davidson, K., Ferguson, G. J., O'Connor, R., Stephens, L. R., and Hawkins, P. T. (2006) Neutrophils from p40phox-/- mice exhibit severe defects in NADPH oxidase regulation and oxidant-dependent bacterial killing. *J Exp Med* **203**, 1927-1937

32.   Goodwin, C. B., Yang, Z., Yin, F., Yu, M., and Chan, R. J. (2012) Genetic disruption of the PI3K regulatory subunits, p85alpha, p55alpha, and p50alpha, normalizes mutant PTPN11-induced hypersensitivity to GM-CSF. *Haematologica* **97**, 1042-1047

33.   Yang, Z., Kondo, T., Voorhorst, C. S., Nabinger, S. C., Ndong, L., Yin, F., Chan, E. M., Yu, M., Wurstlin, O., Kratz, C. P., Niemeyer, C. M., Flotho, C., Hashino, E., and Chan, R. J. (2009) Increased c-Jun expression and reduced GATA2 expression promote aberrant monocytic differentiation induced by activating PTPN11 mutants. *Mol Cell Biol* **29**, 4376-4393

34.   Neel, B. G., Gu, H., and Pao, L. (2003) The 'Shp'ing news: SH2 domain-containing tyrosine phosphatases in cell signaling. *Trends in biochemical sciences* **28**, 284-293

35.   Gu, H., Botelho, R. J., Yu, M., Grinstein, S., and Neel, B. G. (2003) Critical role for scaffolding adapter Gab2 in Fc gamma R-mediated phagocytosis. *J Cell Biol* **161**, 1151-1161

36.   Keilhack, H., David, F. S., McGregor, M., Cantley, L. C., and Neel, B. G. (2005) Diverse biochemical properties of Shp2 mutants. Implications for disease phenotypes. *J Biol Chem* **280**, 30984-30993

37.   Guyton, K. Z., Liu, Y., Gorospe, M., Xu, Q., and Holbrook, N. J. (1996) Activation of mitogen-activated protein kinase by H2O2. Role in cell survival following oxidant injury. *The Journal of biological chemistry* **271**, 4138-4142

38.   Torres, M., and Forman, H. J. (1999) Activation of several MAP kinases upon stimulation of rat alveolar macrophages: role of the NADPH oxidase. *Archives of biochemistry and biophysics* **366**, 231-239

39.   Laplante, M. A., Wu, R., El Midaoui, A., and de Champlain, J. (2003) NAD(P)H oxidase activation by angiotensin II is dependent on p42/44 ERK-MAPK pathway activation in rat's vascular smooth muscle cells. *Journal of hypertension* **21**, 927-936

40.   Makni-Maalej, K., Chiandotto, M., Hurtado-Nedelec, M., Bedouhene, S., Gougerot-Pocidalo, M. A., Dang, P. M., and El-Benna, J. (2013) Zymosan induces NADPH oxidase activation in human neutrophils by inducing the phosphorylation of p47phox and the activation of Rac2: involvement of protein tyrosine kinases, PI3Kinase, PKC, ERK1/2 and p38MAPkinase. *Biochemical pharmacology* **85**, 92-100

41.   Pollock, J. D., Williams, D. A., Gifford, M. A., Li, L. L., Du, X., Fisherman, J., Orkin, S. H., Doerschuk, C. M., and Dinauer, M. C. (1995) Mouse model of X-linked chronic granulomatous disease, an inherited defect in phagocyte superoxide production. *Nature genetics* **9**, 202-209

42.   Kharitonenkov, A., Chen, Z., Sures, I., Wang, H., Schilling, J., and Ullrich, A. (1997) A family of proteins that inhibit signalling through tyrosine kinase receptors. *Nature* **386**, 181-186

43.   Fujioka, Y., Matozaki, T., Noguchi, T., Iwamatsu, A., Yamao, T., Takahashi, N., Tsuda, M., Takada, T., and Kasuga, M. (1996) A novel membrane glycoprotein, SHPS-1, that binds the SH2-domain-containing protein tyrosine phosphatase SHP-2 in response to mitogens and cell adhesion. *Mol Cell Biol* **16**, 6887-6899

44.   van Beek, E. M., Zarate, J. A., van Bruggen, R., Schornagel, K., Tool, A. T., Matozaki, T., Kraal, G., Roos, D., and van den Berg, T. K. (2012) SIRPalpha controls the activity of the phagocyte NADPH oxidase by restricting the expression of gp91(phox). *Cell reports* **2**, 748-755

45.   You, M., Flick, L. M., Yu, D., and Feng, G. S. (2001) Modulation of the nuclear factor kappa B pathway by Shp-2 tyrosine phosphatase in mediating the induction of interleukin (IL)-6 by IL-1 or tumor necrosis factor. *J Exp Med* **193**, 101-110

46.   Chan, R. J., and Feng, G. S. (2007) PTPN11 is the first identified proto-oncogene that encodes a tyrosine phosphatase. *Blood* **109**, 862-867

47.   Liu, X., and Qu, C. K. (2011) Protein Tyrosine Phosphatase SHP-2 (PTPN11) in Hematopoiesis and Leukemogenesis. *Journal of signal transduction* **2011**, 195239

48. Noguchi, T., Matozaki, T., Fujioka, Y., Yamao, T., Tsuda, M., Takada, T., and Kasuga, M. (1996) Characterization of a 115-kDa protein that binds to SH-PTP2, a protein-tyrosine phosphatase with Src homology 2 domains, in Chinese hamster ovary cells. *J Biol Chem* **271**, 27652-27658

49. Kong, X. N., Yan, H. X., Chen, L., Dong, L. W., Yang, W., Liu, Q., Yu, L. X., Huang, D. D., Liu, S. Q., Liu, H., Wu, M. C., and Wang, H. Y. (2007) LPS-induced down-regulation of signal regulatory protein {alpha} contributes to innate immune activation in macrophages. *J Exp Med* **204**, 2719-2731

50. Huang, H., Woo, A. J., Waldon, Z., Schindler, Y., Moran, T. B., Zhu, H. H., Feng, G. S., Steen, H., and Cantor, A. B. (2012) A Src family kinase-Shp2 axis controls RUNX1 activity in megakaryocyte and T-lymphocyte differentiation. *Genes & development* **26**, 1587-1601

51. Nabinger, S. C., Li, X. J., Ramdas, B., He, Y., Zhang, X., Zeng, L., Richine, B., Bowling, J. D., Fukuda, S., Goenka, S., Liu, Z., Feng, G. S., Yu, M., Sandusky, G. E., Boswell, H. S., Zhang, Z. Y., Kapur, R., and Chan, R. J. (2013) The protein tyrosine phosphatase, Shp2, positively contributes to FLT3-ITD-induced hematopoietic progenitor hyperproliferation and malignant disease in vivo. *Leukemia* **27**, 398-408

52. Alblas, J., Honing, H., de Lavalette, C. R., Brown, M. H., Dijkstra, C. D., and van den Berg, T. K. (2005) Signal regulatory protein alpha ligation induces macrophage nitric oxide production through JAK/STAT- and phosphatidylinositol 3-kinase/Rac1/NAPDH oxidase/H2O2-dependent pathways. *Molecular and cellular biology* **25**, 7181-7192

53. Dewas, C., Fay, M., Gougerot-Pocidalo, M. A., and El-Benna, J. (2000) The mitogen-activated protein kinase extracellular signal-regulated kinase 1/2 pathway is involved in formyl-methionyl-leucyl-phenylalanine-induced p47phox phosphorylation in human neutrophils. *Journal of immunology* **165**, 5238-5244

54. Lorenzana, A., Lyons, H., Sawaf, H., Higgins, M., Carrigan, D., and Emanuel, P. D. (2002) Human herpesvirus 6 infection mimicking juvenile myelomonocytic leukemia in an infant. *J Pediatr Hematol Oncol* **24**, 136-141

55. Moritake, H., Ikeda, T., Manabe, A., Kamimura, S., and Nunoi, H. (2009) Cytomegalovirus infection mimicking juvenile myelomonocytic leukemia showing hypersensitivity to granulocyte-macrophage colony stimulating factor. *Pediatric blood & cancer* **53**, 1324-1326

56. Pinkel, D. (1998) Differentiating juvenile myelomonocytic leukemia from infectious disease. *Blood* **91**, 365-367

16

Figure 1. Zymosan-induced ROS production and the activation of Dectin-1-stimulated signaling molecules in WT mouse PEMs. (**A**) ROS production in 0.01×10^6 PEMs upon zymosan (400 μg/ml) stimulation. (**B**) Immunoblot demonstrating phosphorylation of Syk, Shp2, Erk, and Akt at different time points during zymosan-triggered activation in mouse PEMs. (**C**) ROS production in 0.05×10^6 PEMs upon zymosan (400 μg/ml) stimulation in the absence or presence of Syk inhibitor, R406 (5 μm). (**D**) Immunoblot demonstrating phosphorylation of Syk, Shp2, Erk, and Akt at different time points during zymosan-triggered activation in mouse PEMs in the absence or presence of Syk inhibitor, R406 (5 μm). 10 μg of cell lysate was used in immunoblotting. Assays were performed in triplicate.

Figure 2. Zymosan- or SOZ-induced ROS production and the activation of Dectin-1-stimulated signaling molecules in Shp2$^{f/f}$;Mx1Cre- and Shp2$^{f/f}$;Mx1Cre+ mouse BMMs. (**A**) Flow cytometry demonstrating the expression level of macrophage membrane markers Mac1 and F4/80 in Shp2$^{f/f}$;Mx1Cre- and Shp2$^{f/f}$;Mx1Cre+ BMMs. ROS production in 0.05×10^6 Shp2$^{f/f}$;Mx1Cre- or Shp2$^{f/f}$;Mx1Cre+ BMMs upon zymosan (**B**) or SOZ (**C**) stimulation. (**D**) ROS production compiled from 3 independent experiments, n=3, *p<0.01 for Shp2$^{f/f}$;Mx1Cre+ compared to Shp2$^{f/f}$;Mx1Cre- in response to zymosan or SOZ. (**E**) Phagocytic index. 10,000 cells were analyzed by flow cytometry, and the phagocytic index for each cell type was calculated as described under "Experimental Procedures". (**F**) Representative immunoblot showing NADPH oxidase *phox* protein expression. (**G**) Representative immunoblot demonstrating phosphorylation of Shp2, Syk, Erk, and Akt at different time points during zymosan-triggered activation in Shp2$^{f/f}$;Mx1Cre- and Shp2$^{f/f}$;Mx1Cre+ BMMs.

Figure 3. Expression of Shp2 mutants (Shp2-C463A and Shp2-R32K) leads to reduced zymosan- and SOZ-stimulated ROS production. (**A**) Localization of endogenous Shp2 upon SOZ stimulation, staining with anti-Shp2 (Santa Cruz, SC-280) and Alexa555-goat-anti-rabbit IgG in WT BMMS. Alexa Fluor® 488 phalloidin was used to stain F-actin, which specifies early phagosomes. Arrows and asterisks denote Shp2 accumulation on the phagosome cups and early phagosomes, respectively. Representative images from three independent experiments. (**B**) Structural motifs of YFP-tagged Shp2 constructs. (**C**) Flow cytometry indicating the expression level of YFP-tagged WT Shp2 (black), Shp2-C463A (red), or Shp2-R32K (blue). (**D**) Immunoblot demonstrating expression of YFP-tagged Shp2 and endogenous Shp2 in transduced BMMs expressing YFP-tagged WT Shp2, Shp2-C463A, or Shp2-R32K as well as expression of NADPH oxidase components, gp91^{phox}, p22^{phox}, and p67^{phox}. (**E**) Flow cytometry demonstrating the expression level of macrophage membrane markers Mac1 and F4/80 in the populations of BMMs expressing YFP-tagged WT Shp2, Shp2-C463A, or Shp2-R32K. (**F**) ROS production in BMMs expressing YFP-tagged WT Shp2, Shp2-C463A, or Shp2-R32K compiled from 3 independent experiments, n=3, *p<0.01 for Shp2-C463A v. WT or Shp2-R32K v. WT in response to SOZ or zymosan. (**G**) Distribution of YFP-tagged WT Shp2, Shp2-C463A, or Shp2-R32K during SOZ-induced phagocytosis in BMMs. Arrows indicate the cup of phagosomes, asterisks indicate the internalized phagosomes, bar=5μm.

Figure 4. ROS generation in Shp2D61Y- and Shp2E76K-expressing BMMs. (**A**) Immunoblot demonstrating Shp2 and *phox* protein expression in WT BMMs retrovirally expressing empty vector (MIEG3), WT Shp2, or GOF mutants, Shp2-D61Y and Shp2-E76K. (**B-C**) ROS production in 0.1×10^6 BMMs expressing WT Shp2 or GOF mutants, Shp2-D61Y and Shp2-E76K upon zymosan or SOZ stimulation. (**D**) Localization of WT Shp2 and Shp2-D61Y upon SOZ stimulation, immunofluorescent staining with anti-Shp2 (Santa Cruz, SC-280) and Alexa555-goat-anti-rabbit IgG in WT BMMS. Alexa Fluor® 488 phalloidin (Life technologies) was used to stain F-actin. Arrows and asterisks denote Shp2 accumulation on the phagosome cups and early phagosomes, respectively, bar=5μm.

Figure 5. ROS production and the activation of Dectin-1-stimulated signaling molecules in Shp2D61Y;Mx1Cre- and in Shp2D61Y;Mx1Cre+ mouse PEMs upon zymosan or SOZ stimulation.
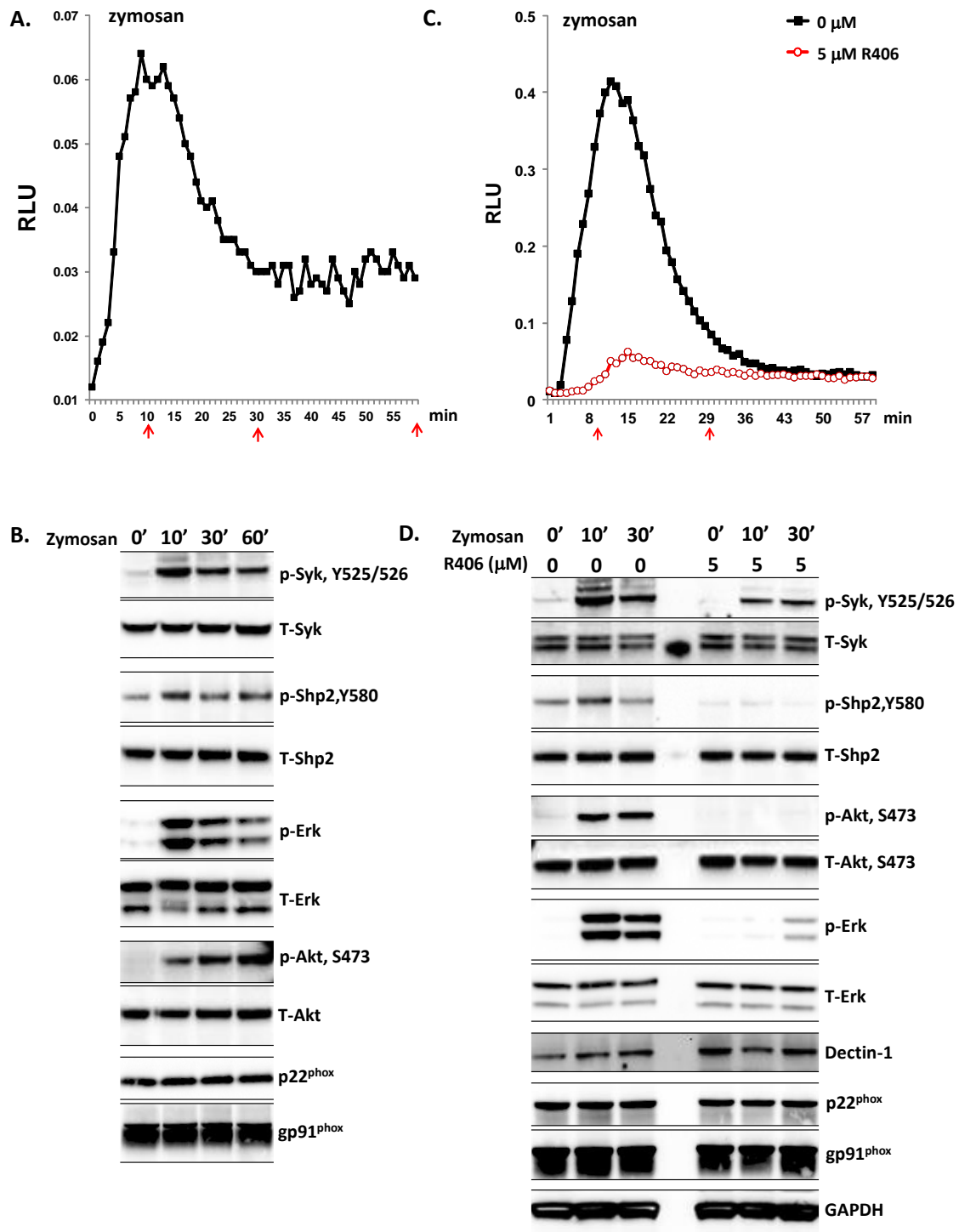
17

(A) Flow cytometry demonstrating the expression level of macrophage membrane markers Mac1 and F4/80 in Shp2D61Y;Mx1Cre- and Shp2D61Y;Mx1Cre+ PEMs. **(B-C)** ROS production in Shp2D61Y;Mx1Cre- and Shp2D61Y;Mx1Cre+ PEMs upon zymosan and SOZ activation. **(D)** ROS production compiled from 3 independent experiments, n=3, *p<0.01 for Shp2D61Y;Mx1Cre+ v. Shp2D61Y;Mx1Cre- in response to zymosan or SOZ. **(E)** Representative immunoblot demonstrating protein level of phosphorylated and total Shp2, Syk, Erk, and Akt as well as *phox* proteins at various time points during zymosan-triggered activation in Shp2D61Y;Mx1Cre- and Shp2D61Y;Mx1Cre+ PEMs.

Figure 6. Erk inhibition reduces zymosan-stimulated ROS production. **(A)** Representative immunoblot demonstrating p-Erk levels during zymosan-triggered activation in the absence and presence of NADPH oxidase inhibitor, Diphenyleneiodonium chloride (DPI) or Erk inhibitor, SCH1772984 (SCH). **(B)** ROS production in 0.1×10^6 WT PEMs in the presence of DPI or SCH. **(C)** ROS production compiled from 3 independent experiments, n=3, *p<0.0001comparing DPI-treated to vehicle-treated, and **p<0.01 for SCH-treated v. vehicle-treated. **(D)** Representative immunoblot demonstrating p-Erk levels in Shp2D61Y;Mx1Cre- and Shp2D61Y;Mx1Cre+ bone marrow-derived macrophages in the absence or presence of Erk inhibitor, SCH1772984 (SCH). **(E)** ROS production in 0.03×10^6 Shp2D61Y;Mx1Cre- and Shp2D61Y;Mx1Cre+ bone marrow-derived macrophages in the absence or presence of SCH. **(F)** ROS production compiled from 3 independent experiments, n=3, *p<0.01 for SCH-treated v. vehicle-treated in Shp2D61Y;Mx1Cre+ cells.

Figure 7. SIRPα phosphorylation and interaction with Shp2 in zymosan-stimulated WT Shp2- and Shp2-C463A-expressing BMMs. **(A)** Co-localization of SIRPα and Shp2 in WT mouse PEMs 10 minutes post zymosan-induced phagocytosis, immunofluorescent staining with anti-SIRPα (Abcam #53721) and anti-Shp2 (BD Bioscience, #610621), and Alexa568-goat-anti-rabbit IgG and goat488-anti-mouse IgG1, respectively. **(B)** Immunoblot demonstrating reduced levels of phospho-SIRPα upon zymosan stimulation of WT PEMs. **(C)** Phosphorylation of SIRPα and Erk in BMMs retrovirally transduced with YFP-WT Shp2 or YFP-Shp2-C463A. Total Shp2, SIRPα, Erk, p22^{phox}, and gp91^{phox} were also examined using antibodies described in the "Experimental Procedures". **(D)** Binding of WT Shp2 and Shp2-C463A mutant to tyrosine phosphorylated SIRPα in macrophages before and post zymosan stimulation. Cell lysates from macrophages expressing YFP-WT Shp2 or YFP-Shp2-C463A were subjected to immunoprecipitation (IP) anti-Shp2 antibody (SC-280, Santa Cruz Biotechnology) followed by immunoblotting (IB) with anti-phospho-SIRPα or anti-Shp2 (#610621, BD Bioscience). 390 μg of protein lysis from macrophages expressing YFP-WT Shp2, and 130 μg of protein lysis from macrophages expressing YFP- Shp2-C463A were used for IP. 10 μg of protein lysis was used to do immunoblot analysis. Data are representative of three separate experiments.
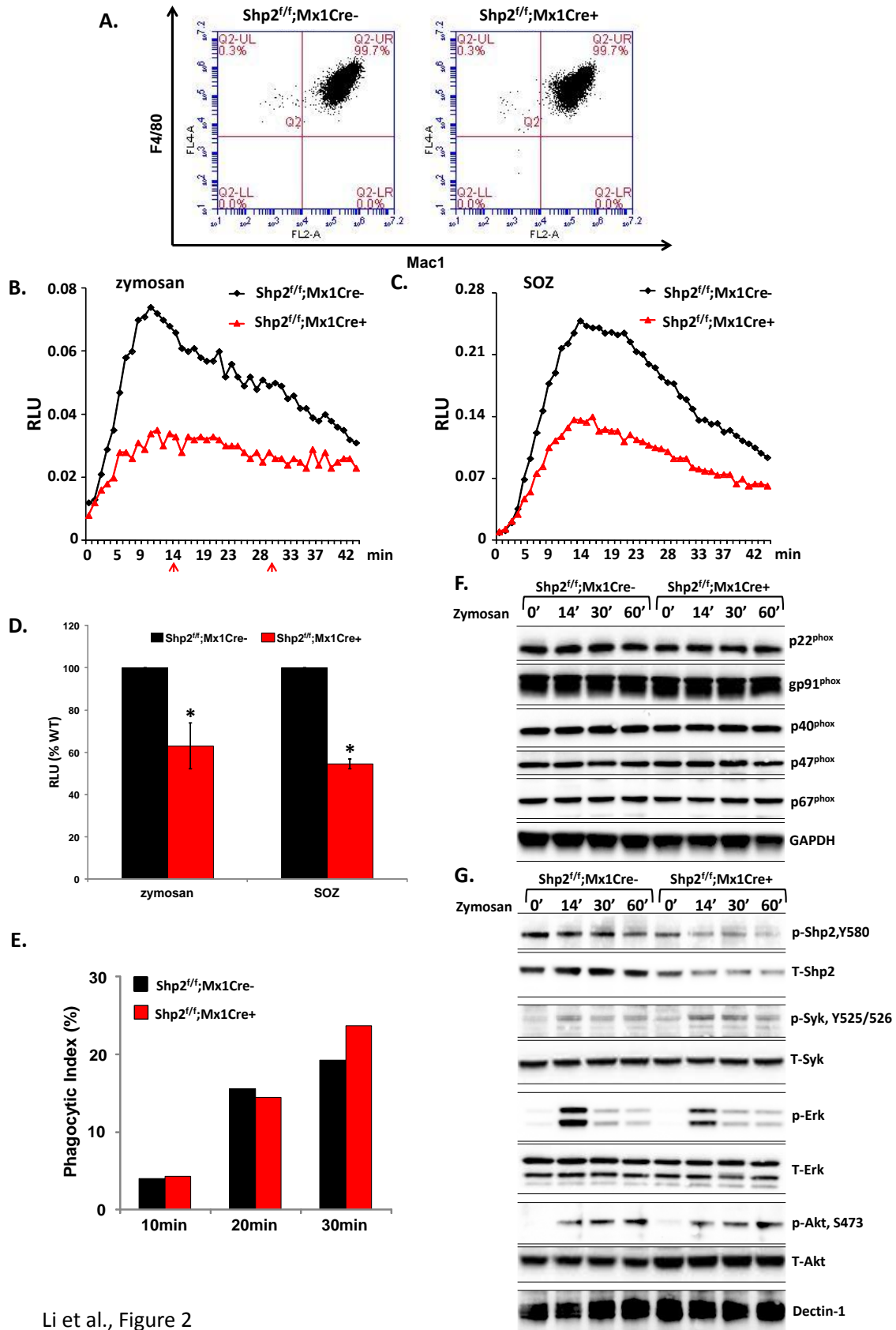
Figure 8. Schematic diagram indicating proposed mechanism of Shp2 and SIRPα interaction in response to Dectin-1 stimulation. **(A)** Cells at resting state. **(B)** Immediate Dectin-1-stimulated ROS production in a Syk-dependent, Shp2-independent manner. **(C)** Following Shp2 dephosphorylation of SIRPα, maximal Dectin-1-stimulated ROS is produced in both a Syk-dependent and Shp2-dependent manner.

18

Li et al., Figure 1

19

A.

B. zymosan

C. SOZ

D.

E.

F.

G.

Li et al., Figure 2

20

A.

Shp2	F-actin	Merge

5μm

B. Shp2-YFP

R32 — N-SH2 — C-SH2 — PTP — C463 — YFP

C.

Count / FL1-A

WT
C463A
R32K

Shp2-YFP

D.

C463A

WT   R32K

Shp2-YFP
Shp2
p22phox
gp91phox
p67phox
β-actin

E.

F4/80 / Mac1

WT   C463A   R32K

C01 1-shp2-yfp-mac1-f4_80 Gate: P1
C04 4-C463A-yfp-mac1-f4_80 Gate: P1
C05 5-R32K-yfp-mac1-f4_80 Gate: P1

F.

RLU (% WT)

■ SOZ
■ zymosan

WT   C463A   R32K

G.

WT Shp2-YFP	Shp2-C463A-YFP	Shp2-R32K-YFP

5μm   5μm   5μm

Li et al., Figure 3

21
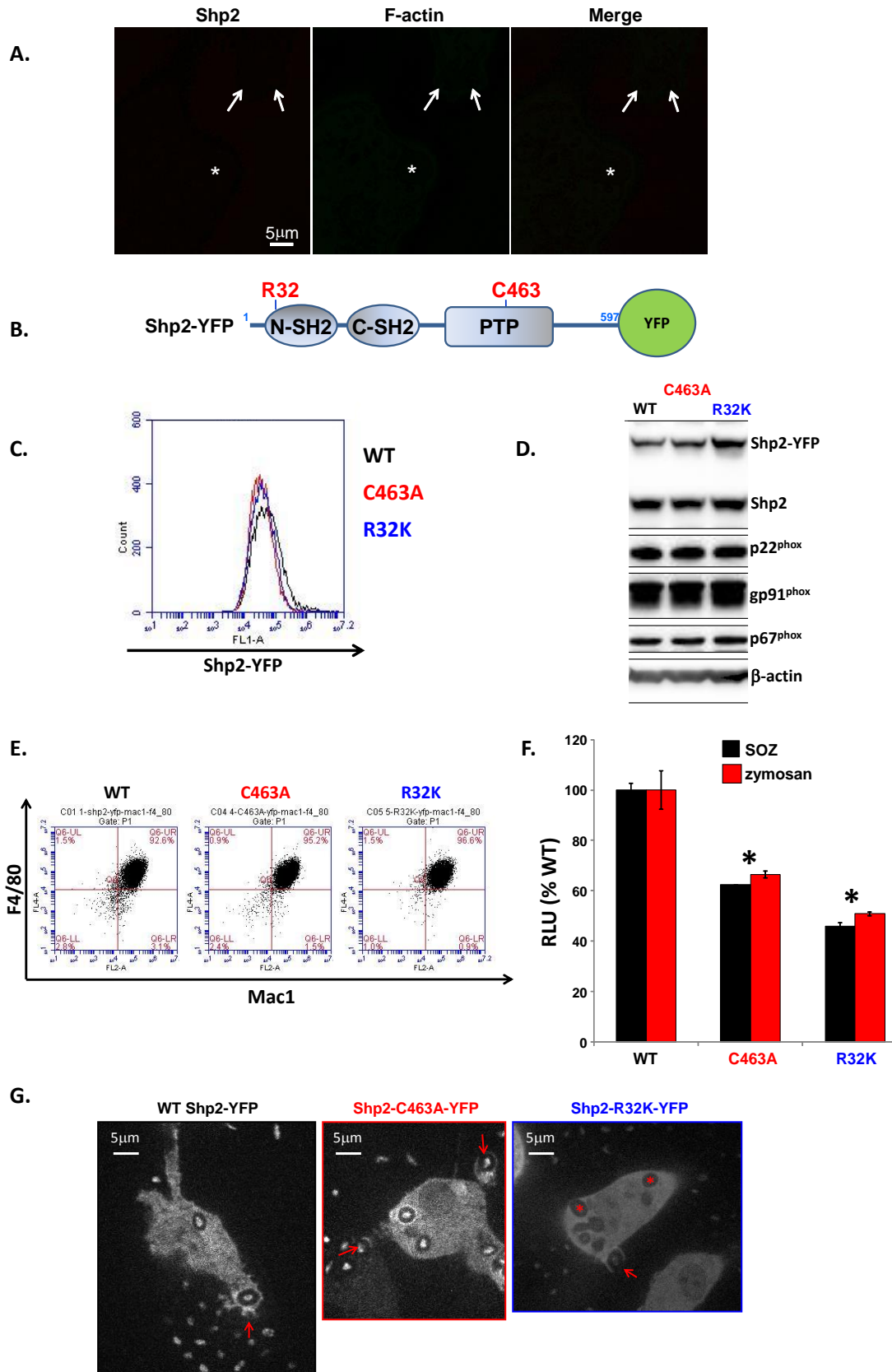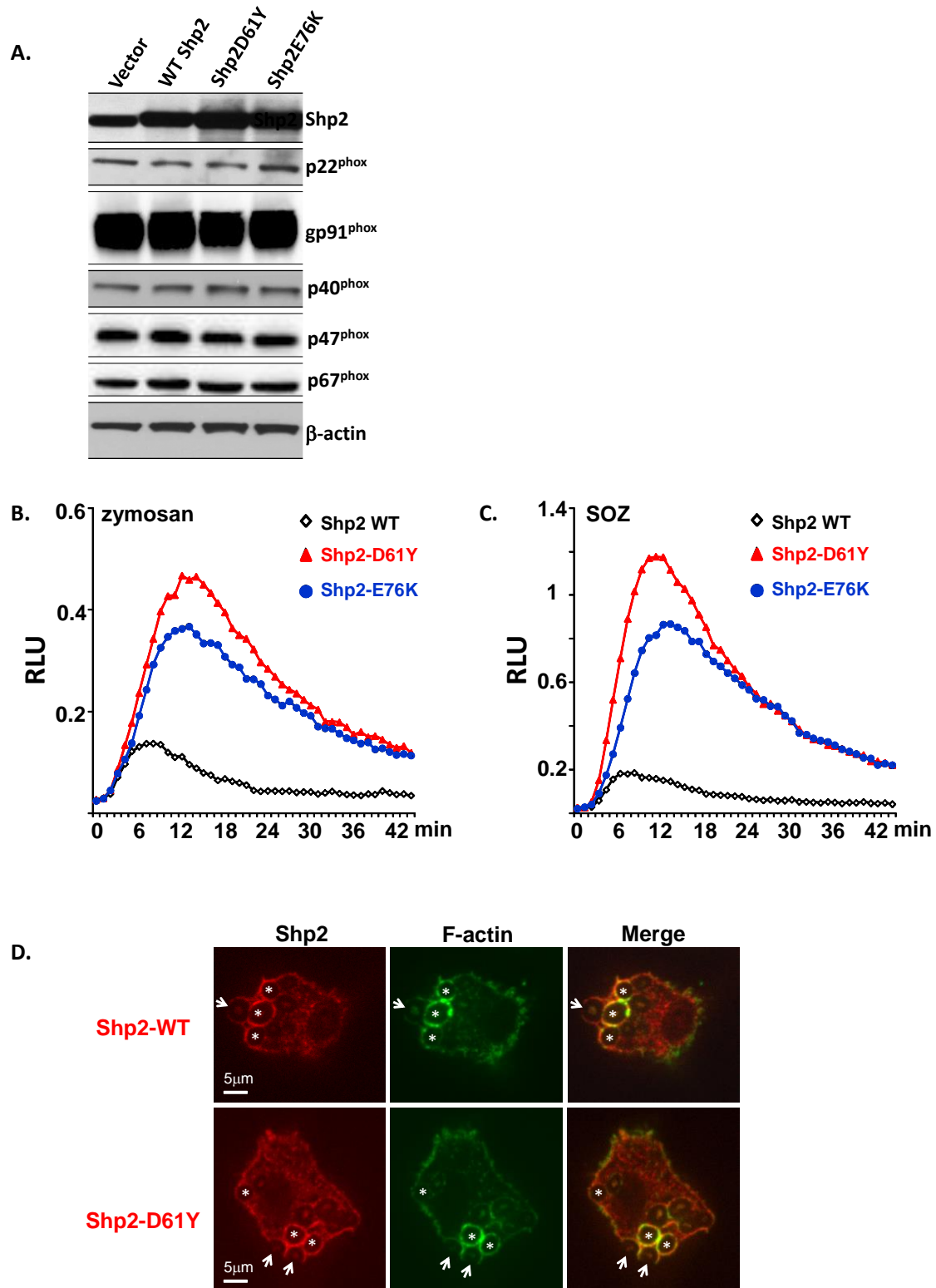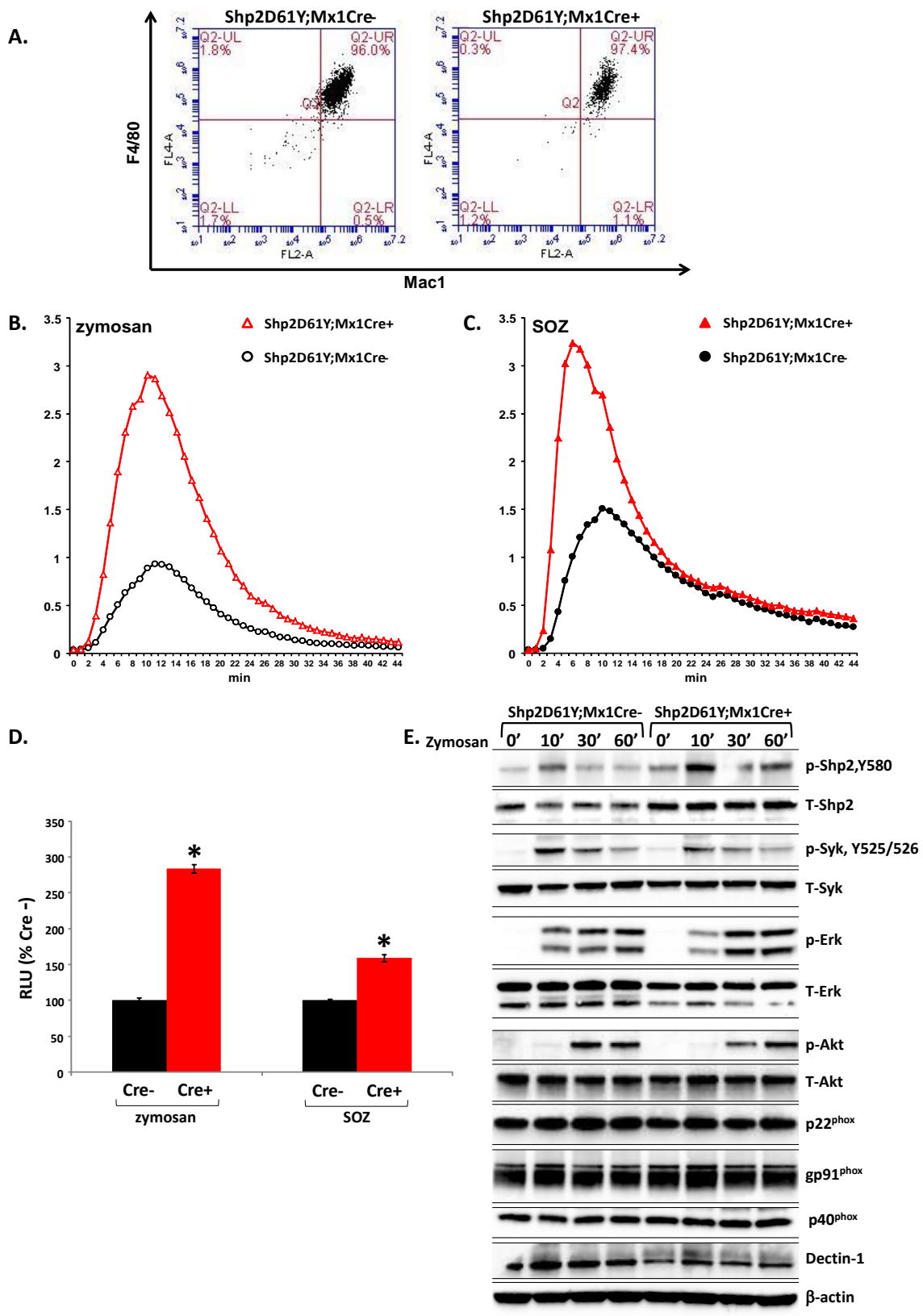
Li et al., Figure 4

Li et al., Figure 5

Li et al., Figure 6

A.

SIRPα	Shp2	Merge

zymosan 10'

zymosan 10'

B.

Zymosan 0' 10' 30' 60'

p-SIRPα

T-SIRPα

GAPDH

C.

WT Shp2-YFP   Shp2-C463A-YFP

Zymosan   0'   14'   0'   14'

p-Erk

T-Erk

Shp2-YFP

Shp2

p-SIRPα

T-SIRPα

p22phox

gp91phox

D.

WT Shp2-YFP   Shp2-C463A-YFP   Beads   WT Shp2-YFP   Shp2-C463A-YFP

Zymosan   0'   10'   0'   10'   0'   10'   0'   10'

IB: p-SIRPα →

IB: Shp2   Shp2-YFP →

Shp2 →

Lysate Input: 390μg   390μg   130μg   130μg   10μg   10μg   10μg   10μg

IP: Shp2   **Lysate**
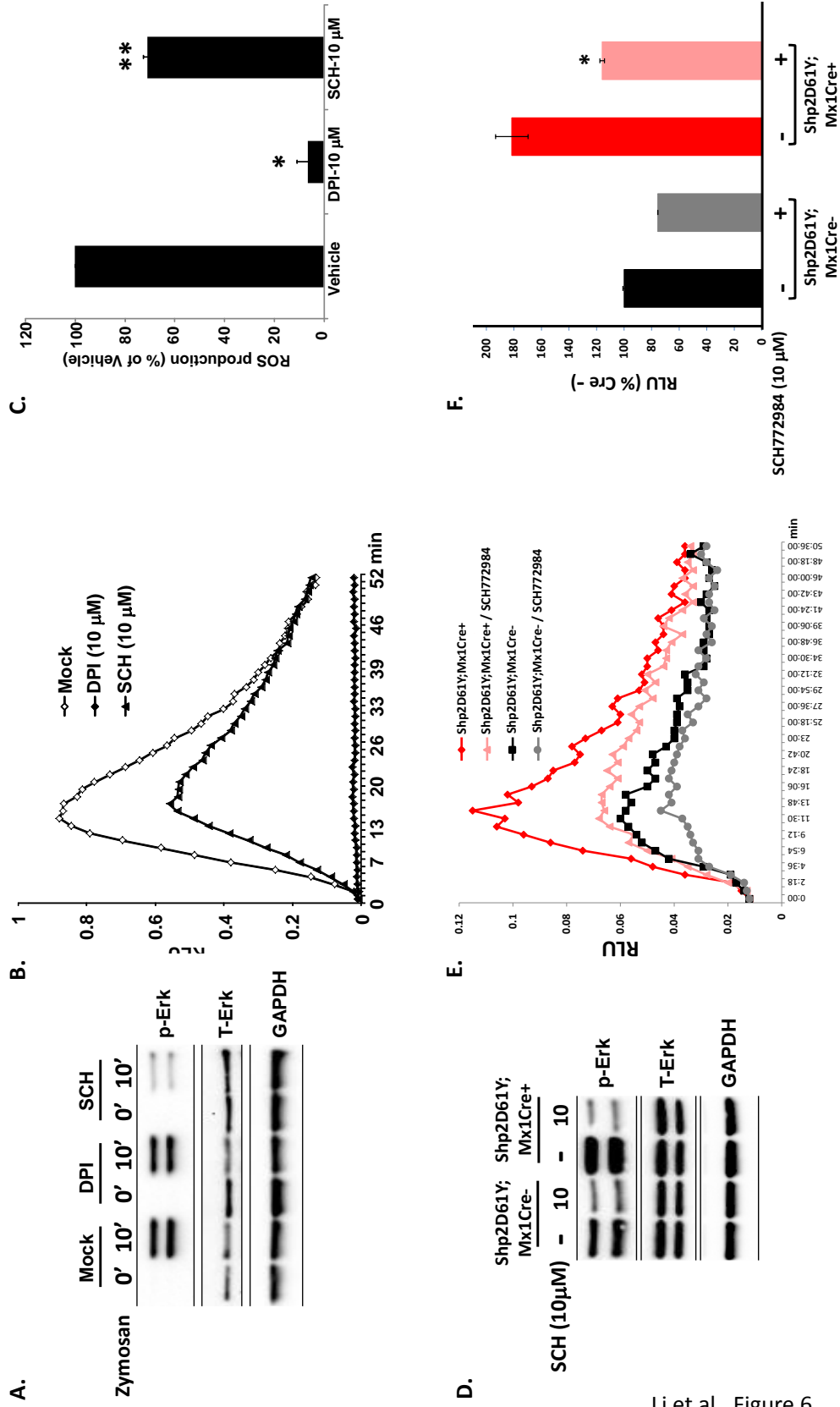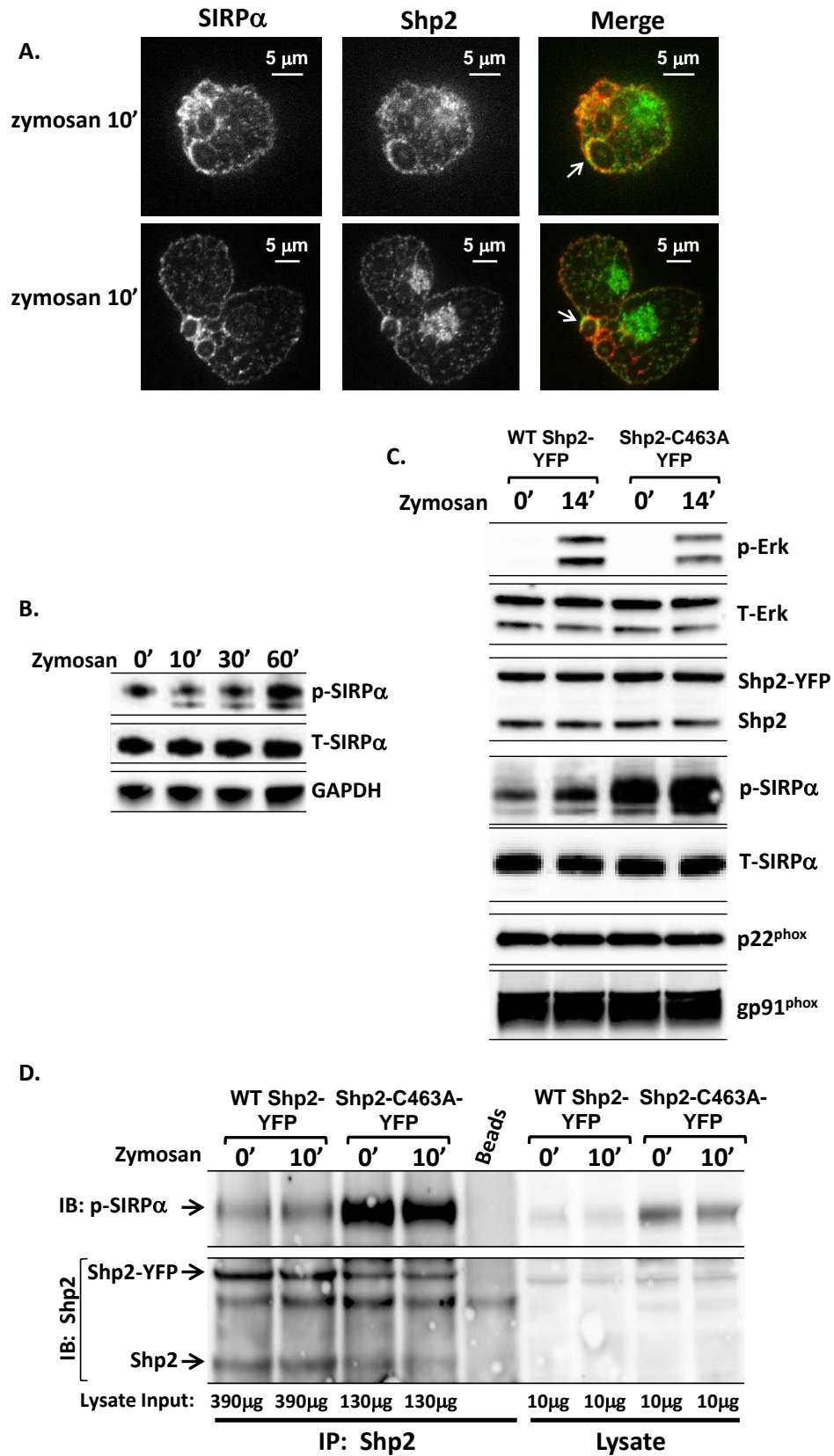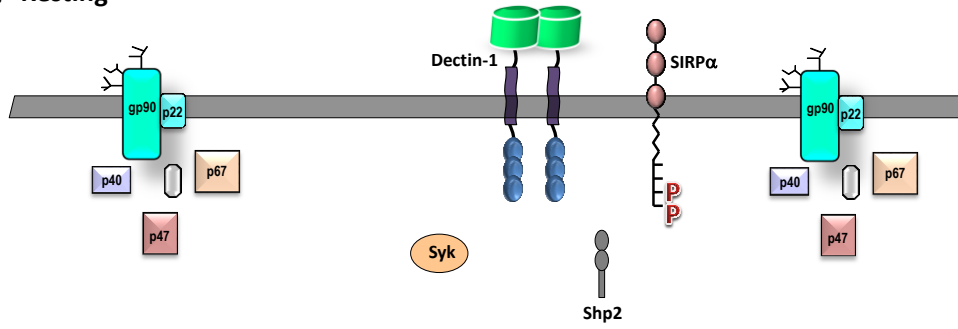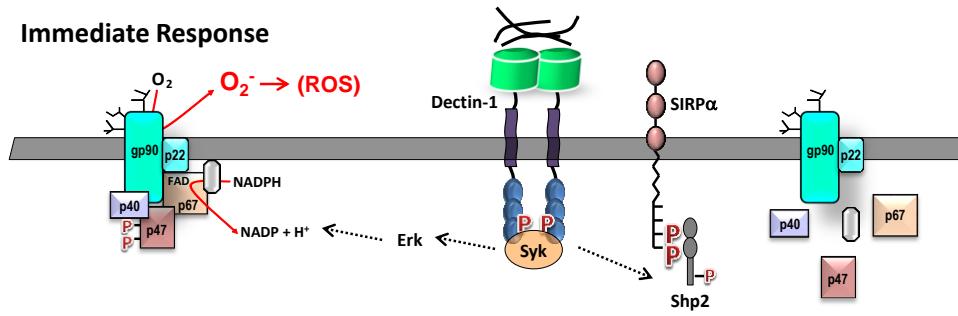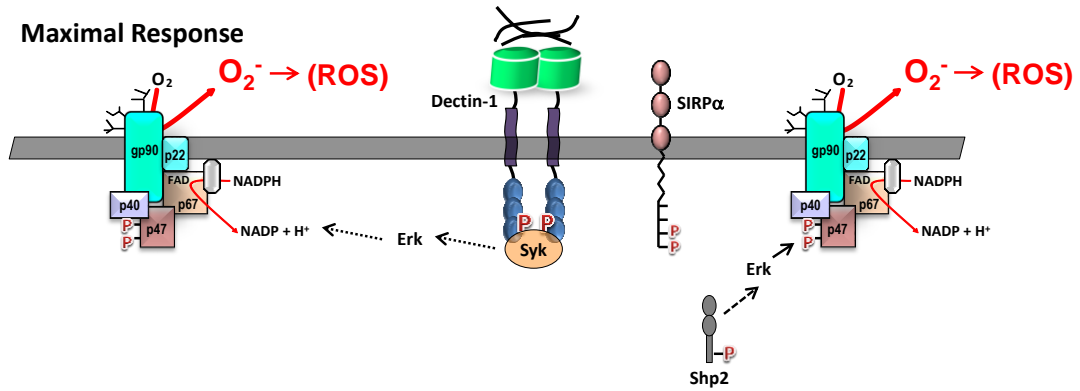
Li et al., Figure 7

Li et al., Figure 8

Molecular Bases of Disease:

Protein Tyrosine Phosphatase, Shp2, Positively Regulates Macrophage Oxidative Burst

MOLECULAR BASES OF DISEASE

CELL BIOLOGY

Xing Jun Li, Charles B. Goodwin, Sarah C. Nabinger, Briana M. Richine, Zhenyun Yang, Helmut Hanenberg, Hiroshi Ohnishi, Takashi Matozaki, Gen-Sheng Feng and Rebecca J. Chan

Find articles, minireviews, Reflections and Classics on similar topics on the JBC Affinity Sites.

Alerts:

- When this article is cited
- When a correction for this article is posted

Click here to choose from all of JBC's e-mail alerts

This article cites 0 references, 0 of which can be accessed free at
http://www.jbc.org/content/early/2014/12/23/jbc.M114.614057.full.html#ref-list-1